C. R. Palevol 10 (2011) 439–452

Contents lists available at ScienceDirect

Comptes Rendus Palevol

www.sciencedirect.com

General palaeontology, systematics and evolution (Micropalaeontology)

Ontogeny of the parietal frill of *Triceratops*: A preliminary histological analysis

Ontogénie de la crête pariétale de Triceratops : une analyse histologique préliminaire

John R. Horner*, Ellen-Thérèse Lamm

Museum of the Rockies, Montana State University, Bozeman, MT 59717, USA

ARTICLE INFO

Article history:
Received 16 November 2010
Accepted after revision 12 April 2011
Available online 29 June 2011

Written on invitation of the Editorial Board

Keywords:
Dinosaurs
Histology
Metaplasia
Hyperostosis

ABSTRACT

The parietal frill of *Triceratops*, one of the largest cranial ornamental features known, undergoes extraordinary morphological changes late in ontogeny — progressing from a large, thickened, solid frill to a substantially larger, thin, fenestrated frill. To understand how this structure changed so dramatically we undertook a histological examination of the caudal end of an ontogenetic series of *Triceratops* parietals. Investigation revealed a histological progression that involved an initial period of non-pathologic hyperostosis, followed by a phase of external (dorsal and ventral sides of the parietal) resorption and border extension, with a conclusive stage hypothesized to be dense fibrous connective tissues mineralized through the process of metaplasia. These fibrous tissues form the caudal end of the mature parietal as well as the epiparietals that fuse to the caudal border of the frill late in ontogeny. Continued resorption near the central parietal regions of the left and right lateral portions of the parietal eventually results in a pair of large circular fenestrae. This progression is somewhat similar to the parietal ontogeny of *Centrosaurus*.

Mots clés :
Dinosaures
Histologie
Métaplasie
Hyperostose

RÉSUMÉ

La crête pariétale de *Triceratops*, l'un des plus grands traits ornementaux du crâne connus, est l'objet d'extraordinaires changements morphologiques tard au cours de l'ontogénie, passant d'une grande crête solide et épaissie, à une crête encore substantiellement plus grande, mince et ajourée. Pour comprendre comment cette structure se modifie si considérablement, nous avons entrepris une analyse histologique d'une série ontogénétique de l'extrémité caudale des pariétaux de *Triceratops*. La recherche révèle une progression histologique qui inclut une période initiale d'hyperostose non pathologique, suivie d'une phase de résorption externe (côtés dorsal et ventral du pariétal) et d'extension de la bordure, avec un stade final supposé constitué de tissus conjonctifs denses et fibreux, minéralisés au cours de processus de métaplasie. Ces tissus fibreux forment l'extrémité caudale du pariétal mature, ainsi que les épipariétaux qui s'amalgament vers la bordure caudale de la crête, tard au cours de l'ontogénie. Une résorption continue vers les zones centrales des portions latérales gauche et droite du pariétal résulte en une paire de grandes ouvertures circulaires. Cette progression est quelque peu similaire à l'ontogénie pariétale de *Centrosaurus*.

1. Introduction

Many non-avian dinosaurs possessed elaborate bony cranial ornamentations such as horns, frills, domes,

* Corresponding author.
E-mail address: jhorner@montana.edu (J.R. Horner).

1631-0683/$ – see front matter © 2011 Académie des sciences. Published by Elsevier Masson SAS. All rights reserved.
doi:10.1016/j.crpv.2011.04.006

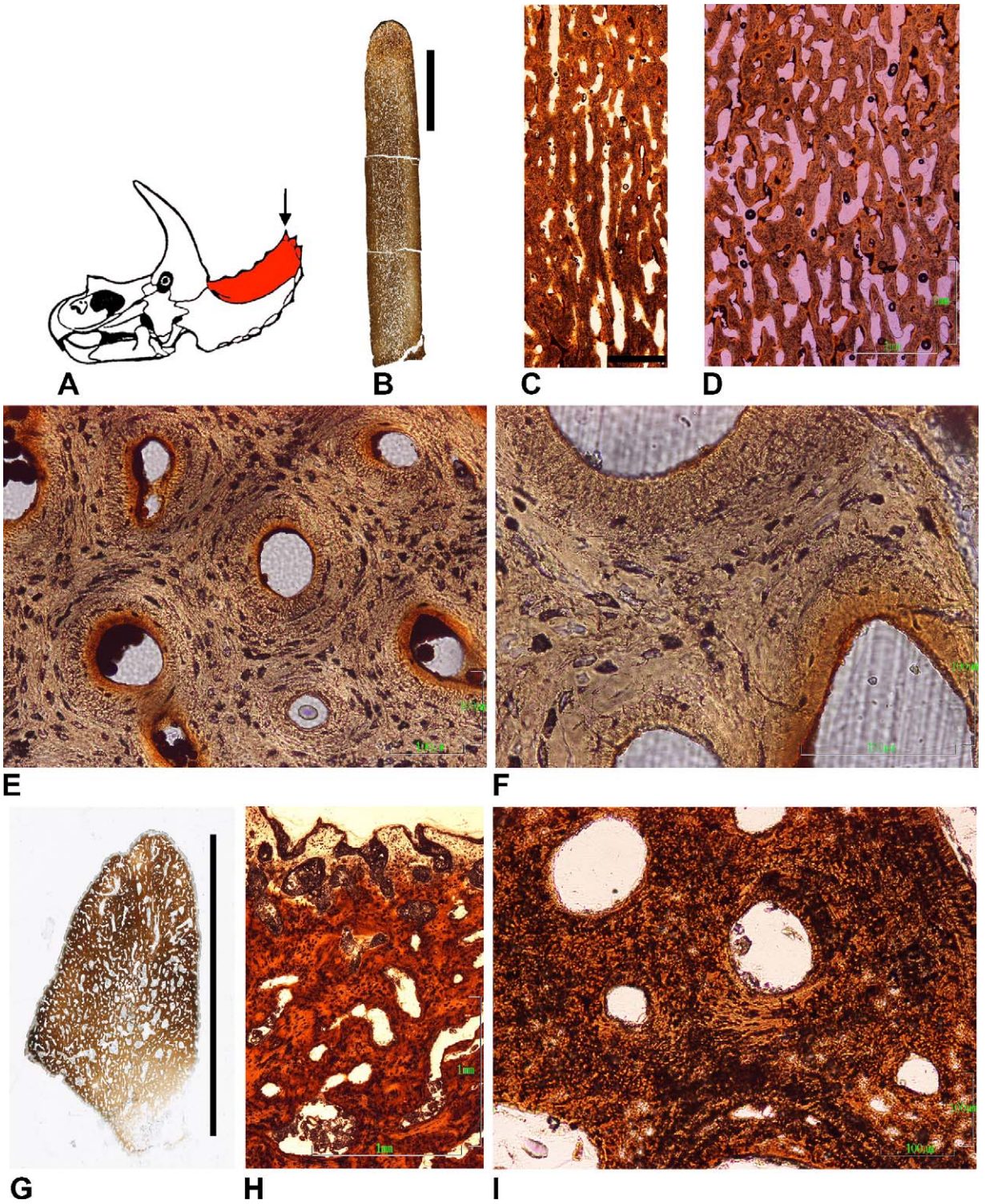

Fig. 1.

and nodes. Although such structures are present in both Saurischia and Ornithischia, the ornithischian group Marginocephalia–which includes the ceratopsids and pachycephalosaurids–developed the most elaborate of these cranial structures. One of the largest of these ornamental structures is the parietal frill of *Triceratops*, a bone that measures more than a meter in length and nearly two meters in width in mature individuals. Interestingly, the morphology of the parietal frill changes dramatically during late ontogeny–transforming from a thickened, solid structure into an elongated, massive shield that is substantially thinner and contains two large fenestrae (Horner and Goodwin, 2006; Scannella and Horner, 2010). To better, understand the ontogenetic progression of morphological events required for these changes to occur we undertook an osteohistological study of the caudal end of the parietal, along with some epiparietal elements.

In a recent, somewhat related study, Tumarkin-Deratzian (2010) examined four parietal frills of the horned dinosaur *Centrosaurus*. The focus of her research was to evaluate the microstructural basis of particular surface textures that had previously been used to assign ontogenetic stages (see Sampson et al., 1997). Tumarkin-Deratzian concluded that the *Centrosaurus* frill initially grew rapidly (evidenced by rostral-caudally oriented radial canals), then, underwent a period of resorption, followed by a second round of osseous accretion in the form of lamellar tissue. Although our study was not focused on evaluating the underlying histology of surface textures, it certainly provided an opportunity to compare the potentially similar microstructural morphology and histology of these two ceratopsians.

2. Materials and methods

Thin-sections were prepared from the caudal ends of five parietals representing various growth stages of *Triceratops,* which includes the adult form originally regarded as *Torosaurus* (see Horner and Goodwin, 2006; Scannella and Horner, 2010). In addition, two isolated epiparietal bones were sectioned (see Table 1). Specimens were acquired from the palaeontology collections of the Museum of the Rockies, Bozeman, Montana, USA (MOR) and the University of California, Berkeley, California, USA (UCMP). The histological slides analyzed in this study are listed in Table 1. Sections were taken from approximately the same location on each parietal and epiparietal (see Fig. 1A), and each was cut in three orientations: sagittal, transverse and coronal (see Supplemental Information for specific descriptions of these orientations).

Many of the fossil specimens were highly porous with unfilled vascular spaces, and some fossils were very soft and fibrous; readily absorbing water even following glue-consolidation and resin-embedding. Due to the atypical composition of this cranial material, many adaptations to standard fossil thin sectioning (Lamm, 2007) were employed (see Supplemental Information).

3. Results

The smallest parietal (*Parietal 1)* (MOR 1199, Fig. 1B–F) is composed exclusively of a cancellous, primary osseous tissue giving the bone a very spongy appearance (Fig. 1B). Although some of the vascular spaces are relatively large, there is no evidence that osteoclasts were involved in expanding the channels, as the borders of these channels are not scalloped. In sagittal section there is an overall radial pattern to the vascular spaces (Fig. 1C), but in coronal view this radial pattern is less distinct (Fig. 1D). In transverse section (Fig. 1E, F), flattened osteocyte lacunae encircling some of the vascular canals suggest the presence of an endosteal centripetal deposit, although upon close inspection (Fig. 1F), there is no evidence of a cementing line, and little evidence of lamellar tissues. Most of the bone has a simple woven texture. The encircling tissues are apparently in the initial-most stages of forming primary osteons. There is no evidence of any resorption or secondary reconstruction.

The smallest epiparietal (*Epiparietal 1*) (UCMP 159233, Fig. 1G–I), measuring two centimeters in height, is very porous, and composed of what appears to be a primary tissue (Fig. 1H), but lacks structures identifiable as osteocyte lacunae. In transverse section (Fig. 1I) each of the vascular channels is simple with no evidence of lamellar tissues. An overall globular appearance of the matrix gives the impression that the section has transverse bundles of fibers, but fibers are not evident in the longitudinal (sagittal) section. Dark areas in the slide apparently represent regions of microbial invasion or possibly a mineral precipitate.

Fig. 1. Juvenile *Triceratops Parietal 1* (MOR 1199) and *Epiparietal 1* (UCMP 159233): *Parietal 1*. A. Drawing of a *Triceratops* skull showing the parietal in red, and the position of the epiparietal bones (black arrow). B and C. Sagittal section of the caudal third of a juvenile *Triceratops* (MOR 1199.Par1-2); B: showing the entire thin-section, (Scale bar of B is 2 cm.); and C: showing predominant radial vascular canals, (Scale bar of C is 1 mm.). D. Coronal section showing the spongy character of the cancellous tissue (MOR 1199.Par1-Cor1). E and F. Transverse section showing the woven tissues with flattened osteocytes circularly oriented around the vascular canals forming initial primary osteons (MOR 1199.Par1-L2). *Epiparietal 1*. G. Epiparietal whole section in sagittal view (UCMP 159233.Epoc1-L4), (Scale bar in G is 2 cm.). H. Sagittal view showing primary tissue (UCMP 159233.Epoc1-L3). I. Epiparietal in transverse view showing fibrous character of tissue with simple vascular canals. Black areas are microbial invasions (UCMP 159233.Epoc1-3).

Fig. 1. Pariétal 1 (MOR 1199) et épipariétal 1 (UCMP 159233) de *Triceratops* juvénile. A. Dessin d'un crâne de *Triceratops* montrant le pariétal en rouge et la position des os épipariétaux (flèche noire). B et C. Section sagittale de la troisième caudale d'un *Triceratops* juvénile (MOR 1199- Parties 1-2) ; B : montrant la section d'ensemble (la barre d'échelle de B est de 2 cm) ; et C : montrant les canaux vasculaires radiaux prédominants (la barre d'échelle de C est de 1 mm). D. Section coronale montrant le caractère spongieux du tissu qui s'oblitère (MOR 1199. Par1-Cor1). E et F. Section transverse montrant le tissus fibreux avec des ostéocytes aplatis orientés de manière circulaire autour des canaux vasculaires, formant les ostéones primaires (MOR 1199.Par1-L2). Épipariétal 1. G. Section d'ensemble de l'épipariétal en vue sagittale (UCMP 159233. Epoc1-L4) (la barre d'échelle de G est de 2 cm). H. Vue sagittale montrant le tissu primaire (UCMP 159233. Epoc1-L3). I. Épipariétal en vue transversale montrant le caractère fibreux du tissu avec de simples canaux vasculaires. Les zones noires représentent des invasions microbiennes (UCMP 159233.Epoc1-3).

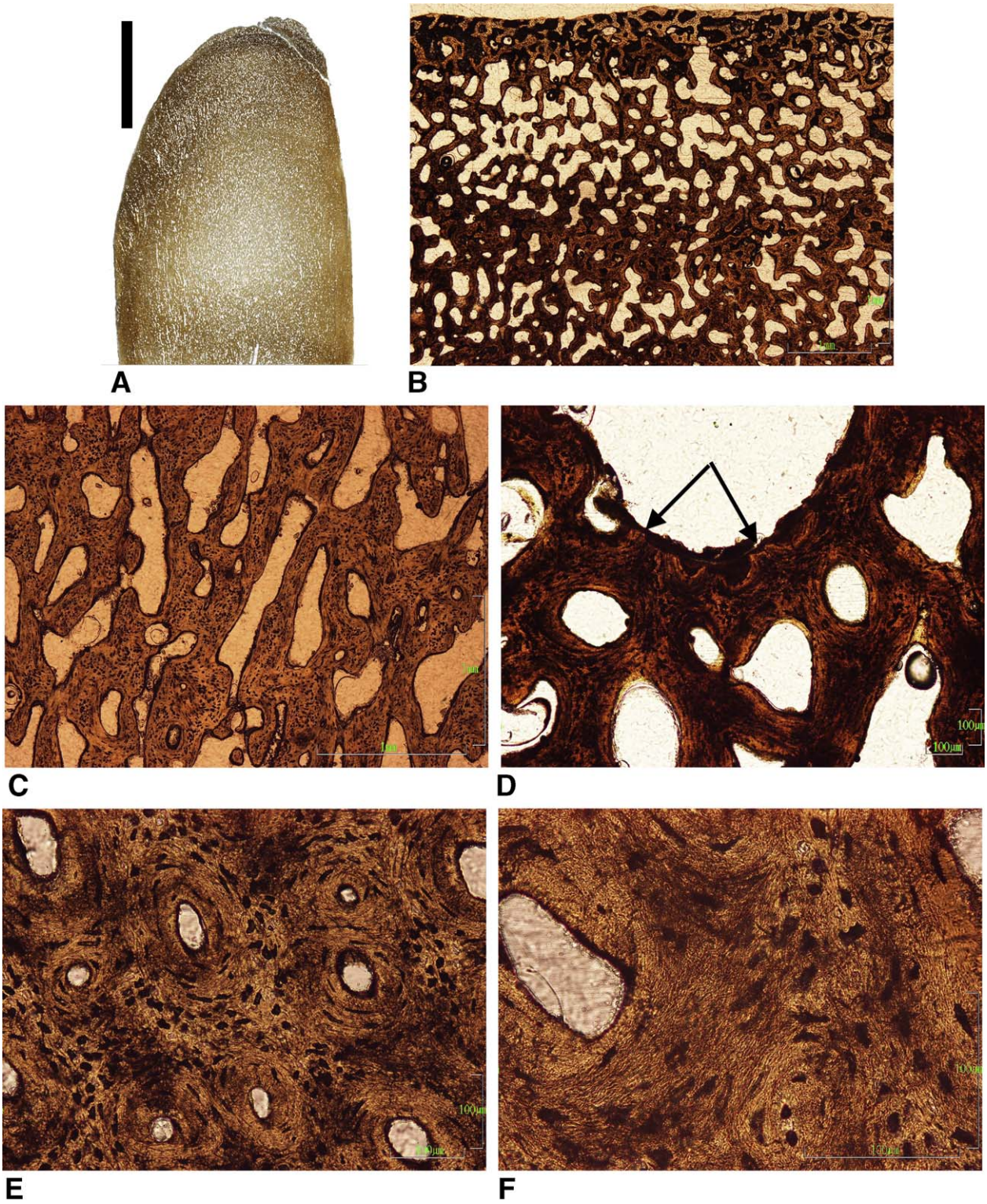

Fig. 2.

Table 1
List of specimens examined in this study.
Tableau 1
Liste des spécimens examinés dans cette étude.

Designation	Museum #	Parietal Length	Thin Section #	Section Orientation	Figure #
Parietal 1	MOR 1199	~ 35 cm	Par1-2 Par1-Cor1 Par1-L2	Sagittal Coronal Transverse	1B,1 C 1D 1E,1F
Epiparietal 1	UCMP 159233	(epiparietal: 2.2 cm)	Epoc1-L4 Epoc1-L3 Epoc1-3	Sagittal Sagittal Transverse	1G 1H 1I
Parietal 2	MOR 2969	~ 60 cm	Par1-1 Par1-Cor1 Par1-L2	Sagittal Coronal Transverse	2A 2B,2 C 2D-2F
Epiparietal 2	MOR 3060	(epiparietal: 5.3 cm)	Epoc1-2 Epoc1-Lat1	Sagittal Transverse	3A-3 C 3D
Parietal 3	MOR 3027	~75 cm	Par1.C-1 Par1.C-L12	Sagittal Transverse	4A-4 C,4F 4D,4E,4G
Parietal 4	MOR 2923	~90 cm	EpiPar1-4 EpiPar1-1	Sagittal Sagittal	5A-5E;6B-6E 6A,6F
Parietal 5	MOR 981	~120 cm	Par1-2 Par1-L2	Sagittal Transverse	7A-F 8A-F

The next larger size parietal (*Parietal 2*) (MOR 2969, Fig. 2A–F) is nearly twice the overall dimensions of the first, and more than twice its dorso-ventral thickness (Fig. 2A). Even though the bone is much larger, the section looks very similar to the smaller individual. The tissue has a very spongy appearance with many radial canals. In coronal section, (Fig. 2B, C) the vascular spaces are large (Fig. 2B), osteocyte lacunae are abundant, and all the tissue is primary with a much woven texture (Fig. 2C). In transverse section, (Fig. 2D–F) one of the large openings is obviously expanded by osteoclasts as evidenced by the crosscutting of primary osteons (Fig. 2D, arrows), but these osteoclastic enlarged spaces are not common. Primary osteons are evident with flattened lacunae encircling the vascular canals (Fig. 2E). Upon magnification, the matrix surrounding many of these vascular spaces is highly fibrous (Fig. 2F).

An isolated epiparietal (*Epiparietal 2*) (MOR 3060, Fig. 3A–D) is the size and shape (see Horner and Goodwin, 2006, 2008) to adorn a parietal frill the size of MOR 2969 (Fig. 2) and has a spongy central region surrounded by a denser, less vascularized exterior (Fig. 3A). In sagittal view the vascularity has a rostral-caudal orientation, and is composed of secondarily reconstructed tissues, as seen in polarized light (Fig. 3B). Near the exterior surface (Fig. 3C) the tissue is very fibrous and contains no evidence of osteocyte lacunae. In transverse section (Fig. 3D), the magnified matrix appears globular where the slide transects bundles of fibers.

The third parietal (*Parietal 3*) (MOR 3027, Fig. 4 A–G) in this study reveals some very interesting differences from *Parietals 1* and *2*. Although *Parietal 3* is fifteen centimeters longer than *Parietal 2*, it is actually dorso-ventrally thinner (Fig. 4A). The majority of the section reveals primary tissues, particularly at the caudal end (Fig. 4B, C), but there is an ontogenetic progression of tissues between the caudal and rostral ends of the sample (contrast the tissues in Fig. 4C [caudal] with those in Fig. 4F). For this reason we have identified the location of the sections that reveal the exterior surface in the image (see letters around Fig. 4A). The section in Fig. 4G was taken from the center of the sample, between locations D and E.

Tissues located at the caudal end (locations B and location C of Fig. 4A) are primarily woven tissues with simple vascular canals. There is fountain-like pattern to the vascular canals as they initially radiate caudally (centrally), but then fan out toward the dorsal and ventral surfaces (Fig. 4B). Hook-like projections point ventrally along the rounded dorso-caudal and ventro-caudal edges (Fig. 4B, C). Resorption (arrows) on both the dorsal and ventral surfaces is evidenced by deep gouges and eroded primary osteons in the mid-section of the sample (Fig. 4D, E, transverse sections). Erosion of secondary osteons is evidenced at the rostral end of the sample (Fig. 4F). Near the center of the sample, between locations D and E (see Fig. 4A), the majority of the tissue is primary (Fig. 4G, transverse section) but protruding through this

Fig. 2. Large juvenile *Triceratops Parietal 2* (MOR 2969). A. Caudal end of parietal showing spongy character with abundant radial canals (MOR 2969.Par1-1), (Scale bar is 2 cm.). B and C. Coronal section showing the spongy character of the cancellous tissue (MOR 2969.Par1-Cor1). D–F. Transverse section (MOR 2969.Par1-L2); D.: showing an erosion room enlarged by osteoclasts as evidenced by truncated canals (black arrows); E: showing structures that look like primary osteons with encircling, flattened osteocytes; and F: showing the fibrous character of the matrix.
Fig. 2. Pariétal 2 de grand *Triceratops* juvénile (MOR 2969). A. Extrémité caudale du pariétal montrant le caractère spongieux, avec d'abondants canaux radiaux (MOR 2969. Par1-1) (la barre d'échelle est de 2 cm). B et C. Section périphérique montrant le caractère spongieux qui s'oblitère (MOR 2969. Par1-Cor1). D–F. Section transversale (MOR 2969. Par 1-L2) ; D : montrant un espace d'érosion élargi par des ostéoclastes, comme le montrent les canaux tronqués (flèches noires) ; E : montrant des structures qui ressemblent à des ostéones primaires, avec des ostéocytes aplatis les encerclant ; et F : montrant le caractère fibreux de la matrice.

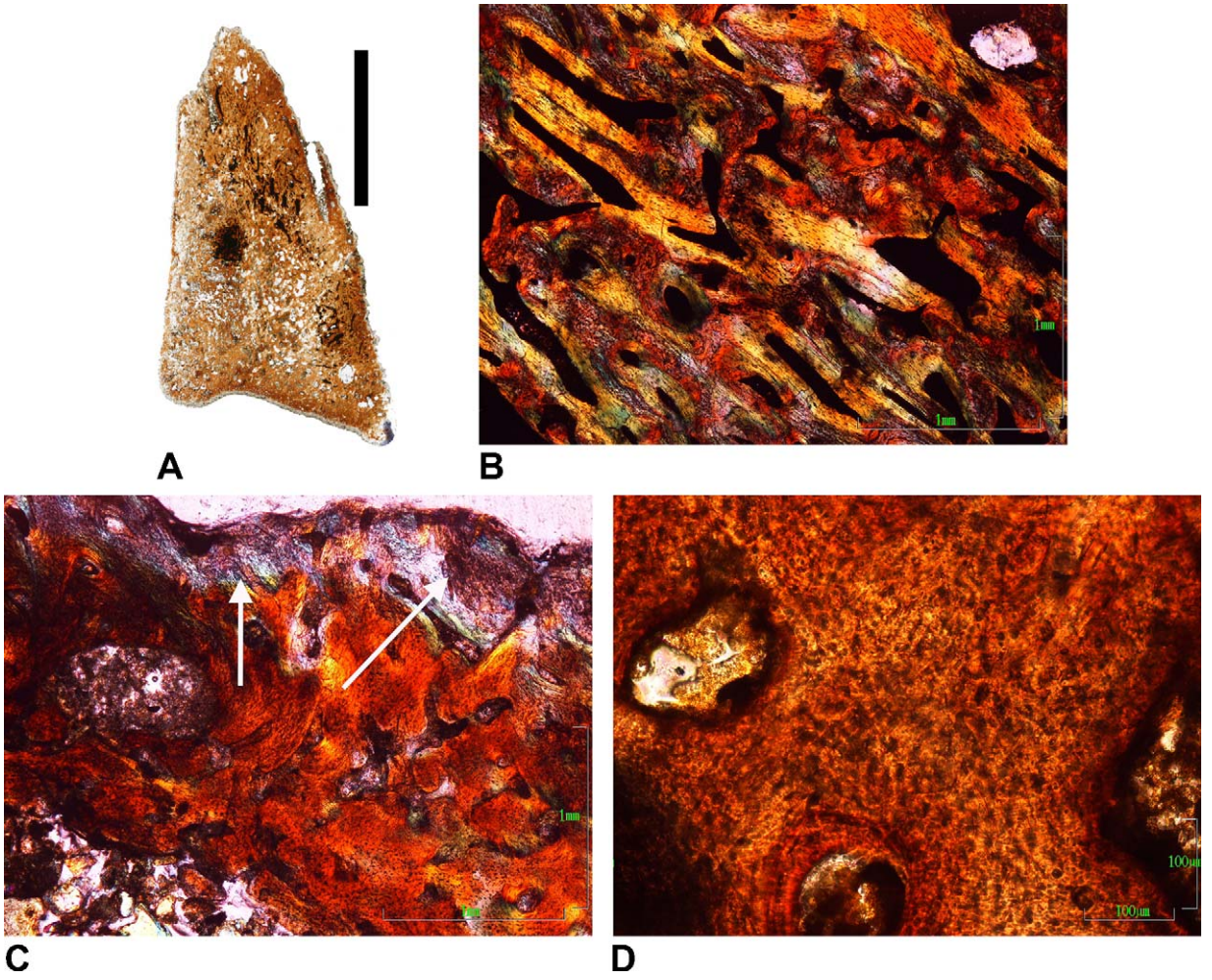

Fig. 3. Large, juvenile *Triceratops Epiparietal 2* (MOR 3060). A–C. Sagittal section (MOR 3060.Epoc1-2). A. Showing spongy character of the whole section. B. In polarized light showing different orientations of tissues as evidenced by the various birefringent colors; and C: showing the fibrous nature of the tissues at the exterior surface (white arrows) (Scale bar of A is 2 cm.). D. Transverse section showing globular looking fiber bundles that are oriented perpendicular to the surface of the slide. Most of the small black structures are mineral filling spaces between the fiber bundles (MOR 3060.Epoc1-Lat1).
Fig. 3. Épipariétal 2 de grand *Triceratops* juvénile (MOR 3060). A–C. Section sagittale (MOR 3060. Epoc1-2). A. Montrant le caractère spongieux révélé par la section d'ensemble. B. En lumière polarisée montrant différentes orientations des tissus, comme le soulignent les couleurs variées de biréfringence ; et C : montrant la nature fibreuse des tissus vers la partie externe (flèches blanches) (la barre d'échelle de A est de 2 cm). D. Section transversale montrant des bouquets de fibres à aspect globulaire, qui sont orientés perpendiculairement par rapport à la surface de la lame. La plupart des petites structures noires sont des espaces remplis de minéraux entre les bouquets de fibres (MOR3060. Epoc1- Lat1).

primary tissue are secondary osteons oriented perpendicular (forming the yellow "Z") to the rostral-caudal length.

Parietal 4 (MOR 2923, Fig. 5A–E), which includes a fused epiparietal (Fig. 6A–F) is derived from a two-meter long skull with a parietal about ninety centimeters in length. Although the epiparietal is fused to the parietal at this stage of ontogeny (Fig. 5A) certain characteristics allow us to determine the delineation of the two elements (Fig. 5B). Primarily we know that the large cavern on the ventral side (left side) represents a channel for a large blood vessel that enters each epiparietal and episquamosal from the ventral side of the parietal. The bases of these vessel channels are indented into the surface of the parietal and squamosals, and form caverns in the epiossifications (Scannella and Horner, 2010).

At this stage the histology of the parietal has changed dramatically in that the tissues are either highly fibrous (Fig. 5C, D) or secondarily remodeled (Fig. 5E). Fiber orientation is not obvious as there are juxtaposing orientations in all regions of the section. In some areas fibers seem to be truncated by vascular openings (center of Fig. 5C), or in some cases the vascular spaces appear to be lined with fiber bundles (central spaces in Fig. 5D). Regardless of whether it is capped by tissues of the epiparietal, the fibrous regions are all located near the external surface of the parietal, which is being resorbed, as evidenced by truncated fibers. This unorganized, highly fibrous tissue is identical to the tissues described as having been mineralized from connective tissues through the process of metaplasia (Main et al., 2005; Ricqlès et al., 2001; Vickaryous and Hall, 2008).

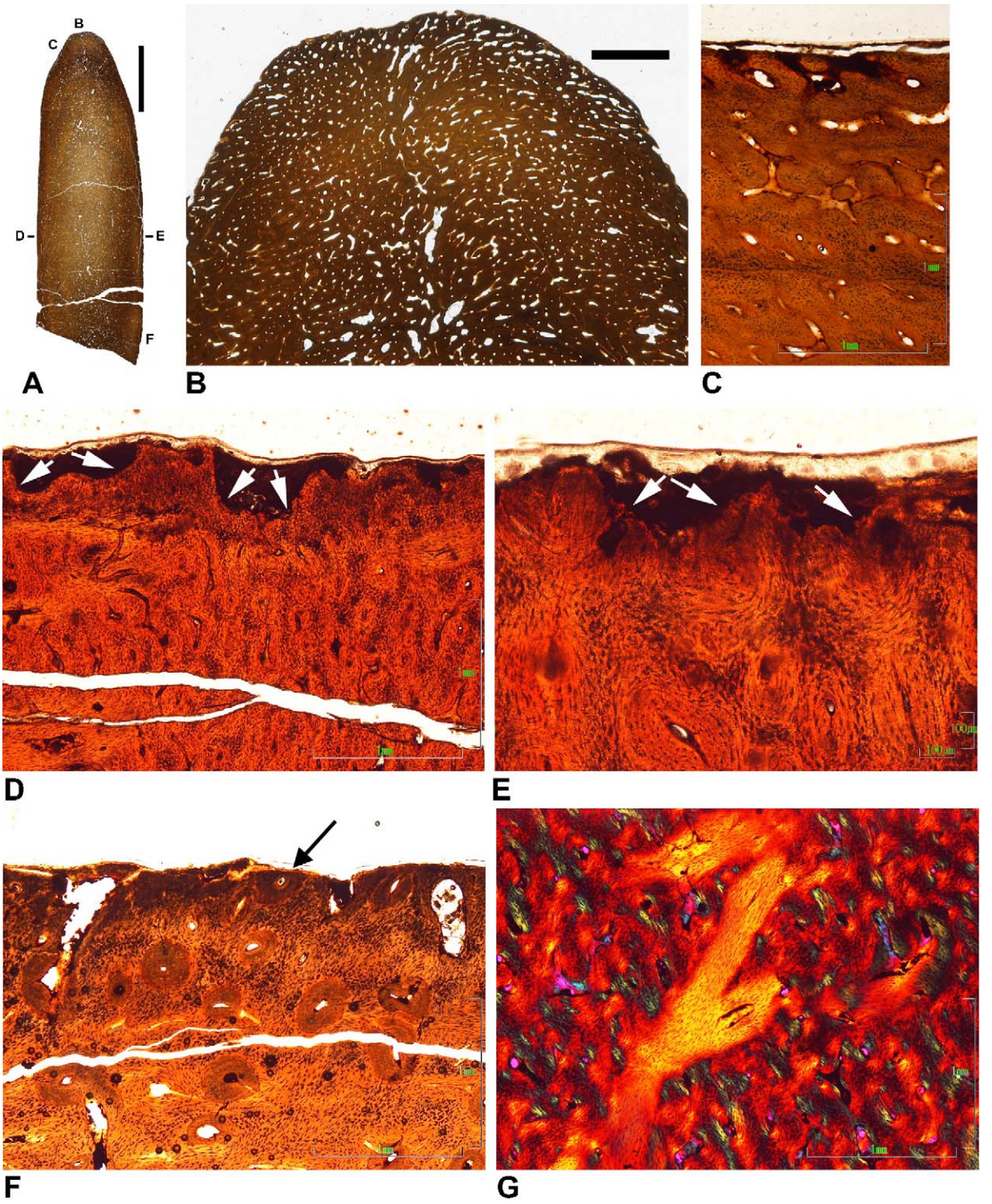
B
C
D
E
F
A
B
C
D
E
F
G

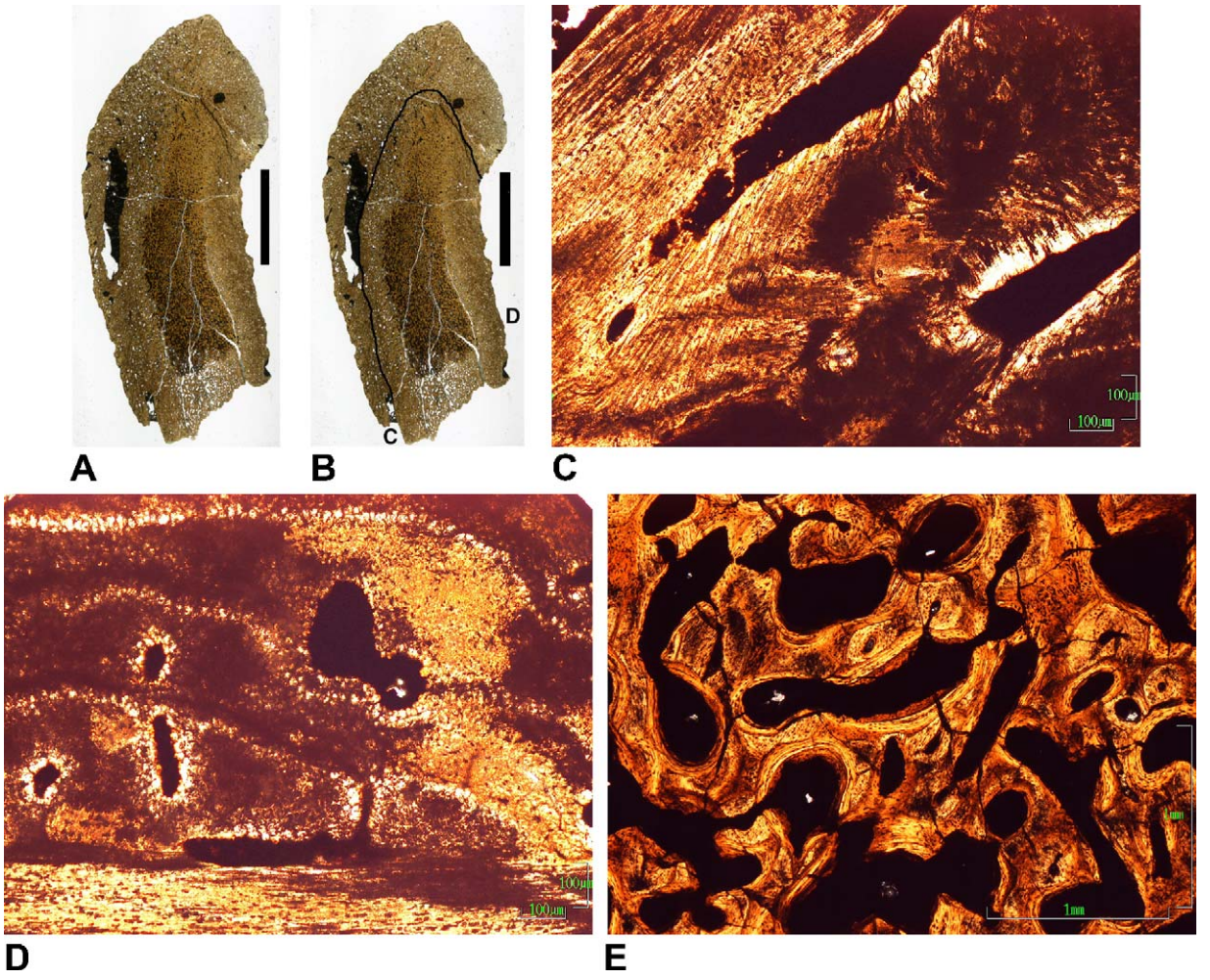

Fig. 5. Large subadult *Triceratops Parietal 4* with attached epiparietal (MOR 2923). A–E. Sagittal section (MOR 2923.EpiPar1-4). A and B. Showing the entire section; B: with a line between the fused epiparietal and parietal, and letters showing the positions of Figures 5C and 5D; dorsal surface is to the right (Scale bars on A and B are 2 cm.). C–E. Images of the parietal portion of the sample; C: showing dense fibers and simple vascular openings near the ventral surface of the parietal; D: dense fibers and simple vascular canals near the dorsal surface of the parietal; and E: showing the highly remodeled interior of the parietal.

Fig. 5. Pariétal 4 de grand *Triceratops*, sub-adulte, avec un épipariétal attaché (MOR 2923). A–E. Section sagittale (MOR 2923. EpiPar1-4). A et B. Montrant la vue d'ensemble de la section ; B : avec une ligne entre pariétal et épipariétal fusionnés et des lettres donnant la position des Figures 5C et 5D ; surface dorsale vers la droite (les barres d'échelle pour A et B sont de 2 cm). C–E. Images de la portion pariétale de l'échantillon ; C : montrant des fibres denses et des ouvertures simples de vaisseaux, près de la surface ventrale du pariétal ; D : fibres denses et canaux vasculaires simples près de la surface dorsale du pariétal ; et E : montrant l'intérieur considérablement remodelé du pariétal.

Fig. 4. Small subadult *Triceratops Parietal 3* (MOR 3027). A–C, F. Sagittal section (MOR 3027.Par1.C-1). A. The whole thin-section with letters showing positions of images B through F (Scale bar of A is 2 cm.). B. The caudal end showing a "fountain-like" pattern of the radial canals fanning out from the center to the rounded caudal border (Scale bar of B is 2 mm.); and C: magnified view of the primary tissues near the caudal end. D and E. Transverse sections (MOR 3027.Par1.C-L12). D. showing resorptive ventral surface (white arrows) and adjacent primary tissues; and E: showing the resorptive dorsal surface (white arrows), and the adjacent primary tissues with mature primary osteons. F. The rostral end of the specimen showing resorption evidenced by erosion of secondary osteons (black arrow) (MOR 3027.Par1.C-1). G. Polarized view of transverse section of the interior of the sample showing a primary tissue with secondary osteons (yellow) oriented latitudinally — perpendicular to the longitudinal rostral-caudal length (MOR 3027.Par1.C-L12).

Fig. 4. Pariétal 3 de petit *Triceratops* sub-adulte (MOR 3027). A–C, F. Section sagittale (MOR 3027. Par1.C-1). A. Vue d'ensemble de la section, avec lettres montrant les positions des images B à F (la barre d'échelle de A est de 2 cm). B. Extrémité caudale montrant une configuration en fontaine des canaux radiaux, émanant depuis le centre jusqu'à la bordure arrondie caudale (la barre d'échelle de B est de 2 mm) ; et C : vue agrandie des tissus primaires vers la terminaison caudale. D et E. Sections transversales (MOR 3027. Part1. C-L12). D. montrant la surface ventrale se résorbant (flèches blanches) et les tissus primaires adjacents ; et E : montrant la surface dorsale se résorbant (flèches blanches) et les tissus primaires adjacents, avec des ostéones primaires matures. F. montrant la terminaison rostrale de l'échantillon indiquent la résorption mise en évidence par l'érosion des ostéones secondaires (flèche noire) (MOR 3027. Part1-C1). G. Section transversale en lumière polarisée de l'intérieur de l'échantillon montrant un tissu primaire, avec des ostéones secondaires (jaunes) orientés latitudinalement – perpendiculaire à l'axe caudo-rostral (MOR 3027. Par1. C-L12).

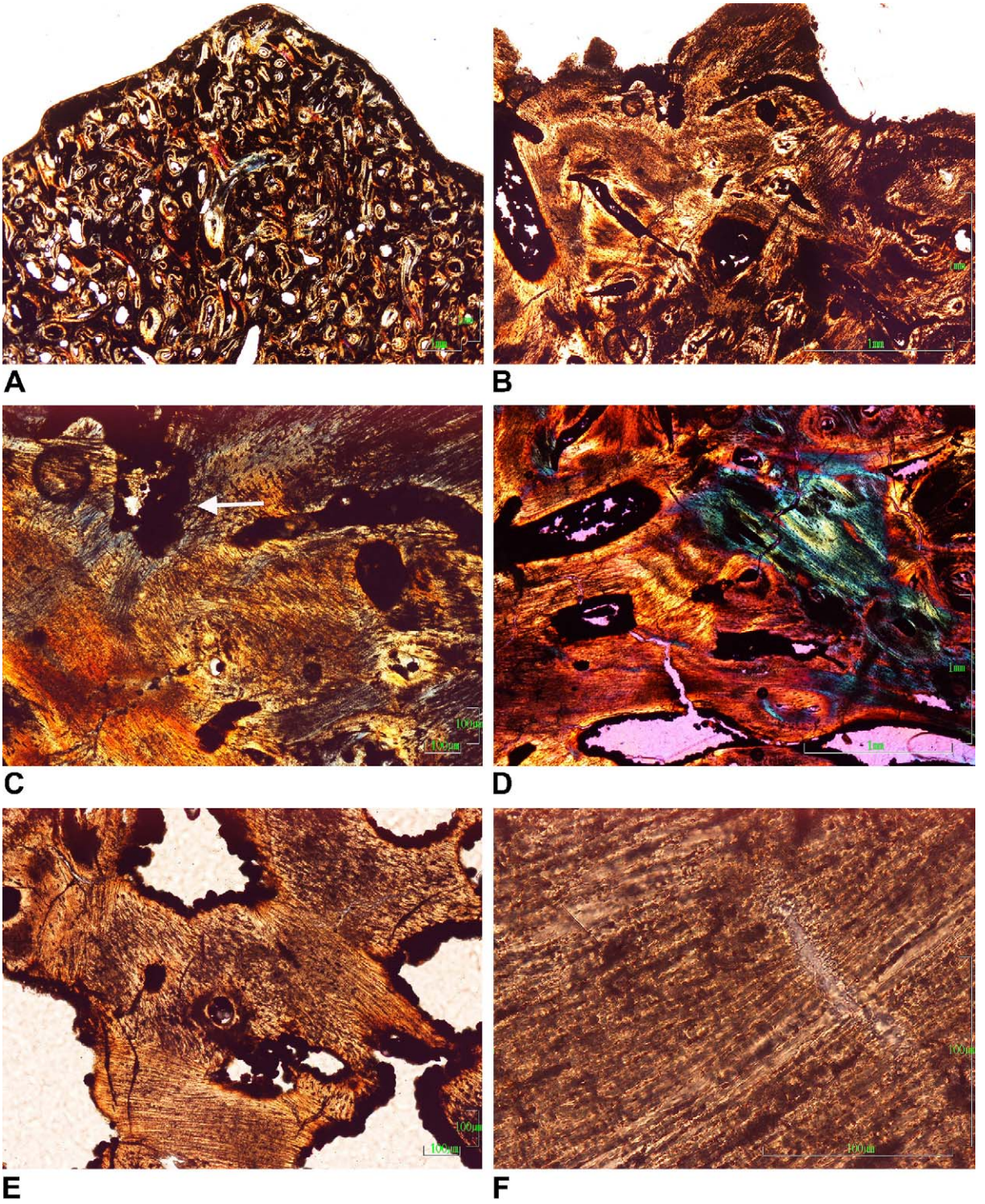

Fig. 6.

The fused epiparietal is primarily composed of secondarily remodeled tissues (Fig. 6A), but a closer inspection, particularly on the dorsal and ventral sides, reveals a zone of highly fibrous tissue with non-oriented fibers (Fig. 6B–F). At the apex of the epiparietal secondary osteons are being resorbed (Fig. 6A). Deeper into the fibrous areas some of the vascular spaces seem to truncate fibers (Fig. 6C, D), and in some cases have scalloped walls (arrow in Fig. 6C). The birefringent pattern in Fig. 6D reflects the various directions of the fiber bundles, and is very similar to the pattern seen in ankylosaur osteoderms (see Main et al., 2005, Fig. 7). The base (rostral-most end on the ventral side) of the epiparietal is highly fibrous with large openings (Fig. 6E), none of which appear to be excavated by osteoclasts. Instead this appears to be a "growing" zone where mineralized tissues are apparently accreting. The borders of these openings are lined with rounded bundles of fibers. As has been described previously (Horner and Goodwin, 2008), the epiparietals and episquamosals change shape considerably during ontogeny. These elements start out as tiny triangular bones that inflate into large triangular structures, and then "flatten" down against the caudal edges of the parietal. As they flatten rostrally a portion of the bone seems to be displaced down the ventral edge of the parietal, producing the sagittal shape seen in Fig. 5B (highlighted by the black line). A highly magnified view of these fibers shows no apparent evidence of osteocyte lacunae (Fig. 6F), although it is possible that the lacunae are flattened and hidden within the fibers.

Parietal 5 (MOR 981, Figs. 7A–F, 8A–F) thin-sections were taken at a location between epiparietals, and therefore lack epiparietal tissues. The caudal tip of the parietal is highly fibrous (Fig. 7B, arrow), and although there are black structures that have the general appearance of osteocyte lacunae, they lack canaliculli, and are actually spaces between fiber bundles. On the ventral side of the section near the caudal end (Fig. 7B) the fiber bundles are arranged in a pattern that resembles herringbone (Fig. 7C). At other locations rostrally, and on both the dorsal and ventral sides, dense Haversian tissues are being resorbed at the surfaces (Fig. 7D, E, arrows). In the central area of the parietal, the tissues are all secondarily reworked, but in some intervening areas between the exterior surfaces and the central core (Fig. 7F), there are regions in which secondary osteons (red), identified by encircling cement lines, reside in a primary matrix that is highly fibrous (green). The fibers are generally oriented in a rostral-caudal direction (the caudal direction is toward the upper left corner of the image).

In transverse section (Fig. 8A–D) these secondary osteons (Fig. 7F) show up as elongated birefringent structures (Fig. 8B, green). The long axes of these Haversian systems are therefore oriented laterally, parallel to the caudal edge of the parietal. The transverse section through the fibrous matrix (the green background of Fig. 7F) shows what at first glance looks like fibrolamellar tissue with embedded osteocyte lacunae and dark parallel zones (Fig. 8C), but the black banding is actually composed of layered, vertically oriented fiber bundles (white arrows). At the base of the dark layered fiber bundles are thin light colored lines that contain very little fiber (yellow arrows). A closer examination of the matrix between the dark fiber bands reveals a very globular, fibrous texture (Fig. 8D), with lacunae (black structures) in between (Fig. 8E, F). This population of lacunae vary greatly in shape and size, and the identification of their progenitor cells (osteoblasts or fibroblasts) is therefore questionable. The vascular canals are all simple.

4. Discussion

Parietal 1 and Parietal 2 are composed of a cancellous, primary osseous tissue that contains an abundance of radially oriented vascular canals. Tissues with these characteristics are described as being the product of hyperostosis (see Francillon-Vieillot et al., 1990, page 495), and known to exist in the skulls of pachycephalosaurid dinosaurs during initial stages of growth (Francillon-Vieillot et al., 1990; Goodwin and Horner, 2004; Reid, 1996). Quantitative studies of the relationship between growth rates and tissue types of extant birds have established that radial fibrolamellar bone tissues are deposited very rapidly (de Margerie et al., 2002; de Margerie et al., 2004). The frill not only expanded rapidly in length and width, but inflated to a dorso-ventral thickness of more than four centimeters, greater than twice the thickness of the mature adult frill. As seen in the parietals of the subadults (*Parietal 3 and Parietal 4*) and adult (*Parietal 5*), following initial inflation of the parietal, external resorption and internal compaction occurred concurrent with continued growth in length and width. The secondary osteons, oriented perpendicular to the rostral-caudal length of the parietal (Fig. 4F, G), show that secondary reconstruction (osteoclastic resorption forming internal erosion rooms) followed the

Fig. 6. Epiparietal portion of *Parietal 4* (MOR 2923). A. Sagittal view in polarized light showing the apex of the epiparietal and its secondarily remodeled interior (MOR 2923.EpiPar1-1). B–E. In sagittal view (MOR 2923.EpiPar1-4); B: image showing the ventral side of the epiparietal with dense fiber bundles and a resorptive surface: C: inner fiber bundles and evidence of osteoclastic resorption (arrow); D: in polarized light the birefringent colors show the disorganization of fibrous tissues; and E: the rostral-most end of the epiparietal on the ventral side of the parietal shows what is apparently the most recent part of the epiparietal to have mineralized. F. Magnified sagittal view showing the density of fibers in the fibrous parts of the epiparietal (MOR 2923.EpiPar1-1).

Fig. 6. Portion épipariétale du Pariétal 4 (MOR 2923) ; A. Vue sagittale en lumière polarisée montrant l'apex de l'épipariétal et son intérieur remodelé secondairement (MOR 2923. EpiPar1-1). B–E. En vue sagittale (MOR 2923. EpiPar1-4) ; B : image montrant la partie ventrale de l'épipariétal, avec des bouquets denses de fibres et une surface de résorption ; C : bouquets de fibres internes et traces de résorption ostéoclastique (flèche) ; D : en lumière polarisée, les couleurs de biréfringence montrent la désorganisation des tissus fibreux ; et E : l'extrémité la plus rostrale de l'épiparietal sur la partie ventrale du pariétal montre ce qui est apparemment la partie la plus récemment minéralisée de l'épiparietal. F. Agrandissement en vue sagittale montrant la densité de fibres dans les parties fibreuses de l'épiparietal (MOR 2923.EpiPar1-1).

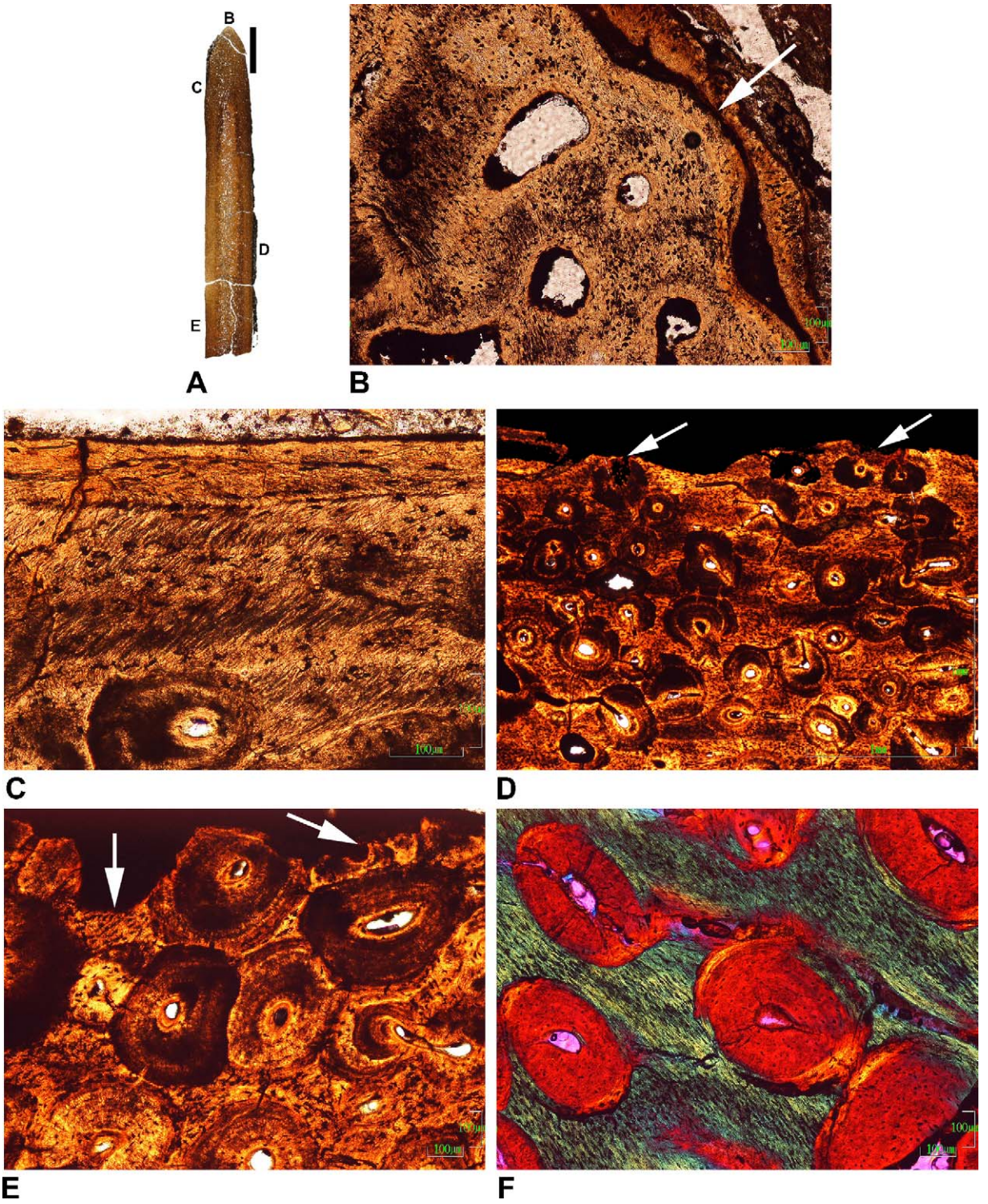

Fig. 7.

widening of the parietal rather than its lengthening. We see that this process continued into adulthood (see Fig. 8B). In the final stages of frill development, when the epiparietals began to fuse to the parietal, the caudal exterior surfaces of the parietal appear to have extended in length through the addition of mineralized connective tissues, possibly formed by metaplasia (see Haines and Mohuiddin, 1968; Vickaryous and Hall, 2008). An abundance of juxtaposing, dense fiber bundles and lack of osteocyte lacunae in the smallest epiparietals (Fig. 1G–I), suggest that these structures may have originated through metaplasia rather than having been formed by osteoblasts.

The light-colored parallel lines (yellow arrows in Fig. 8C) seen in the image showing layers of dense fibers (white arrows in Fig. 8C) near the exterior surface apparently represent "modulations" (see Main et al., 2005, p. 303) of connective tissue metaplasia as described in ankylosaurian osteoderms. Apparently, connective tissues mineralized at the surface, and as successive fiber bands mineralized, the deeper bands were reconstructed. Osteoclasts invaded forming elongated erosion rooms oriented along the rostral-caudal length of the parietal. Haversian reconstruction filled the erosion rooms.

The ontogeny of the *Triceratops* parietal, as interpreted from sections derived from the caudal border, suggests that the parietal frill of juveniles grew rapidly (based on the abundance of radial canals) through a process of non-pathologic hyperostosis, which created a thickened, cancellous, spongy structure. The over-thickening of the structure was probably the result of selection to produce a large, relatively robust structure in a very short period of time, possibly for *status recognition* (Padian and Horner, 2011). When the parietal reached its maximum thickness, bone apposition became restricted to the growing borders while exterior resorption and internal compaction dorso-ventrally thinned the element. Internal compaction and reconstruction strengthened the structure as it became thinner. External resorption apparently progressed at different rates in different regions of the parietal as evidenced by the eventual dual fenestration of the adult parietal (Scannella and Horner, 2010). As the parietal continued to extend in length and width and to thin dorso-ventrally, the structure was eventually constructed of dense Haversian bone in all regions except at the expanding borders. Final additions to the length of the parietal were made possible by the mineralization of connective tissues (apparently through a process of metaplasia), and the fusion of the epiparietals. Here we hypothesize that the final stage of parietal development was the reshaping of the fused epiparietals to form an apparent metaplastic border to the frill. This hypothesized metaplasia of connective tissues occurred in waves or "modulations" (see Main et al., 2005) evidenced by the bands of vertical fiber bundles paralleling the parietal border.

It is likely that the parietal frill of a mature adult weighed about the same as the frill of a large subadult (adult *Triceratops* previous to the synonomy of *Torosaurus* with *Triceratops* by Scannella and Horner, 2010), meaning that although the parietal frill expanded in length and width, its concurrent thinning and fenestration probably kept the weight stable. The highly fibrous, mineralized (metaplastic) border suggests that the outer edge of the parietal was formed of a dense connective tissue. Most of the frill, however, consisting of a thin, fenestrated, dense Haversian bone tissue would likely have been ill-suited for protection from physical combat (see Farke et al., 2009).

Fig. 7. Adult *Triceratops Parietal 5* (MOR 981). A–F. Sagittal section (MOR 981.Par1-2); A: the whole section with letters showing the position of Figures 7B through 7E (Scale bar of A is 2 cm.); B: showing the caudal end (white arrow) of the parietal, and its dense fibrous matrix (many fibers in cross-section) with simple vascular spaces; C: dense fibrous tissue adjacent to the ventral surface; Note the herringbone pattern, and proximity of the secondary osteons; D: showing evidence of resorption at the dorsal surface (white arrows); E: showing resorption at the ventral surface near the rostral end of the sample (white arrows); and F: in polarized light secondary osteons (red) are embedded in a very fibrous matrix (green) that is oriented parallel to the rostral-caudal length (lower right corner to the upper left corner of the image) of the parietal.

Fig. 7. Pariétal 5 de *Triceratops* adulte (MOR 981). A–F. Section sagittale (MOR 981.Par1-2) ; A : vue d'ensemble de la section, avec lettres montrant la position des Figures 7B à 7E (la barre d'échelle de A est de 2 cm) ; B : montrant l'extrémité caudale (flèche blanche) du pariétal et sa matrice fibreuse dense (de nombreuses fibres sont visibles en section transversale), avec des espaces vasculaires simples ; C : tissu fibreux dense, adjacent à la surface ventrale ; à noter la configuration en chevrons et la proximité d'ostéones secondaires ; D : montrant la trace d'une résorption à la surface dorsale (flèches blanches) ; E : montrant la résorption à la surface ventrale, près de la terminaison rostrale de l'échantillon (flèches blanches) et F : des ostéones secondaires (rouges en lumière polarisée) enrobés dans une matrice très fibreuse (verte) qui est orientée parallèlement à l'axe rostro-caudal (coin inférieur droit à coin supérieur gauche de l'image) du pariétal.

Fig. 8. Adult *Triceratops Parietal 5* (MOR 981). A–F. Transverse section (MOR 981.Par1-L2); A: whole section showing laterally oriented vascular canals in the dark brown tissues nearest the exterior surfaces; dorsal surface is up (Scale bar of A is 2 cm.); B: in polarized light, the green colored structures are longitudinal sections of secondary osteons oriented laterally (perpendicular to the rostral-caudal length of the parietal); C: section near the dorsal surface showing layered bands of fibers (white arrows), and light lines (yellow arrows) interpreted as consecutive mineralization zones (see Ricqlès et al., 2001); D: close-up of the tissues nearest to the surface showing what looks to be a fibrolamellar tissue with osteocytes. Note, however, the globular texture of the tissue; E: a highly magnified view of the small areas resembling osteocytes reveals them to be dark structures or spaces fitted between bundles of fibers cut transversely; and F: an image similar to E, but at the exterior surface showing an extensive amount of visible fibers.

Fig. 8. Pariétal 5 de *Triceratops* adulte (MOR981) ; A–F. Sections transversales (MOR 981.Par1-L2) ; A : section d'ensemble, montrant les canaux vasculaires orientés latéralement dans les tissus brun noir, au plus près des surfaces extérieures ; surface dorsale vers le haut (la barre d'échelle de A est de 2 cm) ; B : en lumière polarisée, les structures colorées en vert sont des sections longitudinales d'ostéones secondaires orientés latéralement (perpendiculaires à l'axe rostro-caudal du pariétal ; C : section près de la surface dorsale montrant des bandes litées de fibers (flèches blanches) et des lignes claires (flèches jaunes) interprétées comme des zones de minéralisation consécutives (voir Ricqlès et al., 2001) ; D : les tissus se referment au plus près de la surface montrant ce qui semble être un tissu fibro-lamellaire avec ostéocytes. À noter cependant la texture globulaire du tissu ; E : le grossissement important des petites zones ressemblant à des ostéocytes les révèle comme étant des structures ou des espaces foncés situés entre des bouquets de fibers coupées transversalement ; et F : une image similaire à E, mais montrant à la surface extérieure une extension abondante de fibers visibles.

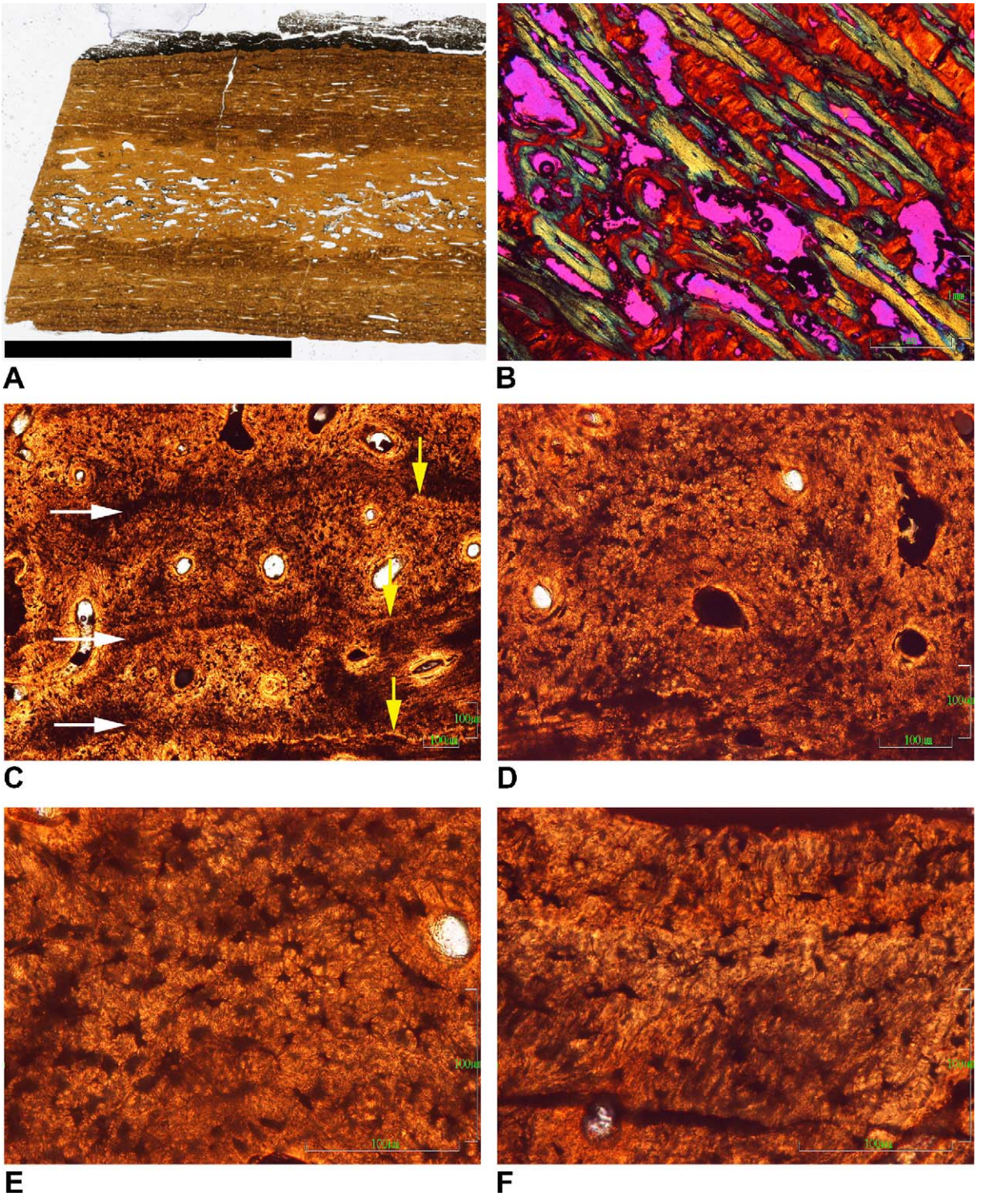

Fig. 8.

Interestingly, the results of this study revealed a great deal of similarity with the results of Tumarkin-Deratzian (2010), in that the ontogenetic growth of the *Triceratops* parietal is similar to the growth of the *Centrosaurus* parietal. In our study, however, we found that the third phase of growth involved mineralization of a dense, fibrous tissue, hypothesized to have formed through metaplasia, whereas Tumarkin-Deratzian suggested the third phase to involve normal lamellar tissues. The accretion illustrated by Tumarkin-Deratzian (2010: Figure 17, 4D, page 257) shows what certainly looks like lamellar bone tissue, but what in *Triceratops* (upon close examination) is actually dense bands of fibers, hypothesized not to have been deposited by osteoblasts, but instead, mineralized from connective tissues. Further comparative osteohistologic studies will be required to resolve whether or not metaplastic processes are involved with the final formation of the centrasaurine frill, or whether its ontogenetic histology is possibly dissimilar to that of *Triceratops*.

This study was preliminary in that it involved the analysis of a few ontogenetic samples from the caudal ends of *Triceratops* parietals. A thorough study is underway in which thin-sections are being taken from various locations on all ornamented bones at different ontogenetic stages of *Triceratops*. Preliminary observations of these sections suggest that growth processes are similar throughout the skull.

Acknowledgements

We gratefully thank Armand de Ricqlès for his friendship and histological guidance over the past three decades. We also thank Mark Goodwin and John Scannella for many valuable discussions on *Triceratops*, Carrie Ancell for her exquisite fossil preparations (prior to destructive histological analyses), Holly Woodward, John Scannella, Alida Bailleul, and Denver Fowler for encouraging us to "cut everything," and our many donors for their continued support of this research. We also greatly appreciate the constructive comments of our reviewers, including Andy Farke, and especially Michel Laurin for his editorial support.

Appendix A. Supplementary material

There is supplementary material associated to the electronic version of the article at doi:10.1016/j.crpv.2011.04.006.

References

Farke, A.A., Wolff, E.D.S., Tanke, D.H., 2009. Evidence of combat in *Triceratops*. PLoS ONE 4 (1), e4252.doi:10.1371.

Francillon-Vieillot, H., de Buffrénil, V., Castanet, J., Géraudie, J., Meunier, F.J., Sire, J.Y., Zylberberg, L., de Ricqlès, A., 1990. Microstructure and mineralization of vertebrate skeletal tissues. In: Carter, J.G. (Ed.), Skeletal biomineralization: patterns, processes and evolutionary trends. , Vol. 1. Van Nostrand Reinhold, New York, pp. 471–530.

Goodwin, M.B., Horner, J.R., 2004. Cranial histology of pachycephalosaurs (Ornithischia: Marginocephalia) reveals transitory structures inconsistent with head-butting behavior. Paleobiology 30 (2), 253–267.

Haines, R.W., Mohuiddin, A., 1968. Metaplastic bone. J. Anat. 103 (3), 527–538.

Horner, J.R., Goodwin, M.B., 2006. Major cranial changes during *Triceratops* ontogeny. Proc. Royal Soc., London B 273, 2757–2761.

Horner, J.R., Goodwin, M.B., 2008. Ontogeny of cranial epi-ossifications in *Triceratops*. J. Verteb. Paleontol. 28 (1), 134–144.

Lamm, E.T., 2007. Paleohistology widens the field of view in paleontology. Proceedings–Microscopy and Microanalysis 13 (Supp 2), 50–51.

Main, R.P., Ricqlès, A. de, Horner, J.R., Padian, K., 2005. The evolution and function of thyreophoran dinosaur scutes: implications for plate function in stegosaurs. Paleobiology 31 (2), 291–314.

Margerie, E. de, Cubo, J., Castanet, J., 2002. Bone typology and growth rate: testing and quatifying "Amprino's Rule" in the Mallard (*Anus platyrhynchos*). C. R. Biologies 325, 221–230.

Margerie, E. de, Robin, J.-P., Verrier, D., Cubo, J., Groscolas, R., Castanet, J., 2004. Assessing a relationship between bone microstructure and growth rate: a fluorescent labeling study in the king penguin chick (*Aptenodytes patagonicus*). J. Exper. Biol. 207, 869–879.

Padian, K., Horner, J.R., 2011. The definition of sexual selection and its implications for dinosaurian biology. J. Zool. 283, 23–27.

Reid, R.E.H., 1996. Bone histology of the Cleveland-Lloyd dinosaurs and of dinosaurs in general, Part 1: Introduction: Introduction to bone tissues. Brigham Young University Geological Studies 41, 25–71.

Ricqlès, A. de, Pereda Suberbiola, X., Gasparini, Z., 2001. Histology of dermal ossifications in an ankylosaurian dinosaur from the Late Cretaceous of Antarctica. Asoc. Paleontol. Argentina. Publication Especial 7, 171–174.

Sampson, S.D., Ryan, M.J., Tanke, D.H., 1997. Craniofacial ontogeny in centrosaurine dinosaurs (Ornithischia: Ceratopsidae): taxonomic and behavioral implications. Zool. J. Linn. Soc. 121, 293–337.

Scannella, J.B., Horner, J.R., 2010. *Torosaurus* Marsh, 1891, is *Triceratops* Marsh, 1889 (Ceratopsidae: Chasmosaurinae): synonomy through ontogeny. J. Verteb. Paleontol. 30 (4), 1157–1168.

Tumarkin-Deratzian, A.R., 2010. Histological evaluation of ontogenetic bone surface texture changes in the frill of *Centrosaurus apertus*. In: Ryan, M.J., Chinnery-Allgeir, B.J., Ebreth, D.A. (Eds.), New perspectives on horned dinosaurs, the Royal Tyrrell Museum Ceratopsian Symposium. Indiana University Press, pp. 251–263.

Vickaryous, M.K., Hall, B.K., 2008. Development of the dermal skeleton in *Alligator mississippiensis* (Archosauria, Crocodylia) with comments on the homology of osteoderms. J. Morphol. 269, 398–422.